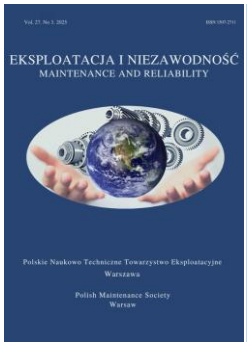

Eksploatacja i Niezawodnosc – Maintenance and Reliability

Volume 27 (2025), Issue 3

journal homepage: http://www.ein.org.pl

Article citation info:
Franek J, Malaka J, Michalski P, Świder J, IIoT based operational technology system for monitoring belt transmissions, Eksploatacja i Niezawodnosc – Maintenance and Reliability 2025: 27(3) http://doi.org/10.17531/ein/197382

IIoT based operational technology system for monitoring belt transmissions

Indexed by: Web of Science Group

Jakub Franek[a,*], Julian Malaka[a], Piotr Michalski[a], Jerzy Świder[b]

[a] Faculty of Mechanical Engineering, Silesian University of Technology, Poland
[b] KOMAG Institute of Mining Technology, Poland

Highlights

- Lower number of measurements necessary to determine the parameters of the drive system.
- According to Industry 4.0 standards, system based on the Industrial In-ternet of Things.
- Multiplatform, integrated information technology system.
- Generating data on the basis of various, distributed sources.
- Industrial hardware and software facilities, adjusted to Ethernet-based networking.

Abstract

The aim of the presented research is to study concepts of identifying anomalies in the operation of synchronous belt transmissions. Consideration was given to the possibility of reducing the number of measurements necessary to determine the key parameters of the drive system. According to Industry 4.0 standards, the prototype of such a system is based on the Industrial Internet of Things. The proposed solution is a multiplatform, integrated information technology, generates data on the basis of various, distributed sources. The system combines standard industrial hardware and software facilities, adjusted to Ethernet-based networking. The expected result was a graphical data representation accessible in digital displays, acquired from the computational nodes (e.g. cloud). Thus, it is possible to extend the field of experiments to analyse the condition of transmission operation - all this is possible thanks to the developed and studied assembly techniques and IT connections, as well as algorithms and automation in data acquisition and processing.

Keywords
diagnostics, drive system, Industry 4.0, belt transmission, IIoT.

1. Introduction

The need for monitoring motion of pulleys of synchronous belt transmissions in the context of the transmission diagnosis possibilities is not a novel concept. As early as 1983, it was observed that the generation of synchronisation error in the operation of a toothed belt transmission is influenced by the interference of the toothed belt and pulley in the area of their meshing [1]. This has been also described in a series of scientific publications [2-7]. It was shown that anomalies, such as damage to the belt material in the form of tooth loss or inadequate belt preload levels, are identifiable from the time courses of the divergence between the angular velocities of the pulleys [8-13]. The results of these studies were models linking the form of periodic changes in the error values with specific causes of their occurrence: irregularities in the assembly or operation of the drive [4, 14-17]. Force interactions such as a belt tensioner operation or contact between pulley and belt surfaces were identified as asynchronism factors [18-20]. All above can influence the life-time of the belt [21-23].

(*) Corresponding author.
E-mail addresses: J. Franek (ORCID: 0009-0000-1591-4014) jakufra047@student.polsl.pl, J. Malaka (ORCID: 0000-0002-0681-2734) julian.malaka@polsl.pl, P. MIchalski (ORCID: 0000-0002-6924-4009) piotr.michalski@polsl.pl, J. Świder (ORCID: 0000-0002-4310-0373) jerzy.swider@polsl.pl,

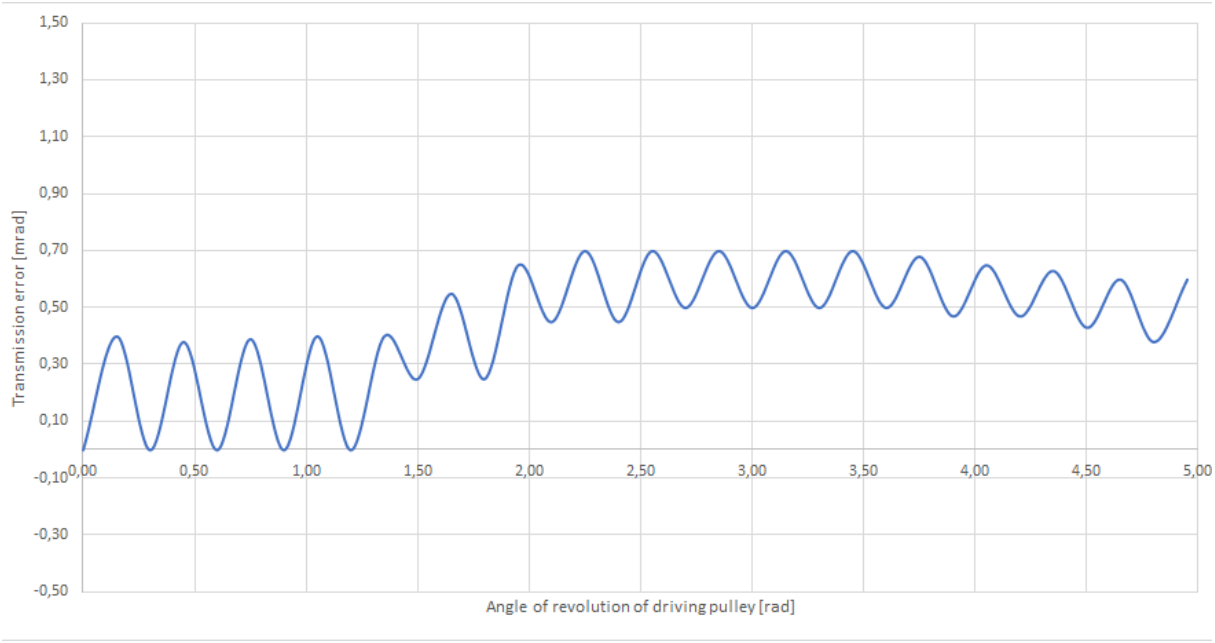

Fig. 1. Plot of transmission asynchronism during incomplete meshing [1].

The authors of this publication have noticed a lack of knowledge in the area of correlation between the error of the pulleys' velocity values with other important phenomena – vibrations. This is a phenomenon related to the centrifugal force, which is transmitted to all the elements of the drive [24-27]. This can lead to temporary separation of the belt and pulley surfaces in areas where this should not occur. The same can happen in the area of belt contact with the tensioner pulley. In addition, vibration-induced belt waving will cause a temporary change in the tension force of the belt, which is adjusted in the standard way by the spring tensioner. The deformation of the free oscillating toothed belt section will affect the motion of the other belt sections that are meshed with the pulleys [28]. In energy terms: the vibrations will absorb some of the energy that is supplied from the motor directly in mechanical form, and any loss of energy will reduce the level of performance of the drive shaft on the driven side [15]. It is assumed that the level of the belt and pulley material wear can also cause errors in the transmission process, reflected in the measurements.

However, before the research on modelling correlations between wear level and kinematic phenomena as well as the influence of vibrations on pulley position and speed courses can be conducted, the information generating system must be designed, and its industrial usability proved experimentally. It is the object of the described study. It was crucial for the authors to develop an *industry-ready* system for conducting further industrial research to study various industrially applied transmissions in their operation in practical conditions. Thus, the *plug-and-play* functionality was important and its realisation was to be achieved by meeting IIoT standards for easy IT/OT integration of the system with digital industrial technology (distributed components of the system connected by TCP/IP, scalability of the system, platform independents source codes) as well as installation ease and adaptiveness (standardised hardware and mounting in the proposed diagnostic system).

1.1. Concept of solution

It is assumed that such a system should provide basic data for classical diagnostic purposes:

- vibration level measured in bearing nodes,
- angular speed of pulleys,
- angular position of pulleys,

as well as indicators for synchronisation error measurements:

- differences between rotational speeds of pulleys,
- differences between positions of pulleys,
- and indicators of correlation between parameters of pulley motion as well as vibration and synchronisation error for research purposes.

According to Industry 4.0 standards, the prototype of such a system, described hereinafter, is based on the Industrial Internet of Things (IIoT). The proposed solution is

a multiplatform, integrated information technology, generating data based on various, distributed sources. Various measurement methods are required as well, thus the system combines standard industrial hardware and software facilities, adjusted to Ethernet-based networking. The expected result is a graphical data representation accessible in digital displays, acquired from a computational node (e.g. cloud).

Taking into account industrial production conditions, in which systems improving the operation and diagnostics of drives are of particular value, the considerations were guided by the criterion of minimum instrumentation and manual intervention in the processes of identification and elimination of operating anomalies. Consideration was given to the possibility of reducing to a minimum the number of measurements necessary to determine the key parameters of the drive system. The research cross-sectionally analysed the possibility of identifying selected anomalies in the operation of synchronous belt transmission:

- synchronisation error,
- vibrations.

The focus of this paper is on improving methods of monitoring these parameters and finding correlations between them.

2. Materials and methods

This chapter describes a laboratory drive model, which has been analysed in terms of its ability to implement a system for generating the information described earlier. Computational methods are also presented, which, according to the authors' assumptions, are expected to lead to desired diagnostic and test indicators.

2.1. Hardware configuration of test bench

The test bench consists of the components shown in Fig. 2, which are listed and described in detail in Table 1.

A diagram of the mechanical linkage is shown in Fig. 3. The drive shaft is mounted so that it is possible to install an additional load in the form of a flywheel with a mass of 4 kg and with its centre of gravity offset from the axis of rotation, which causes vibrations in the system.

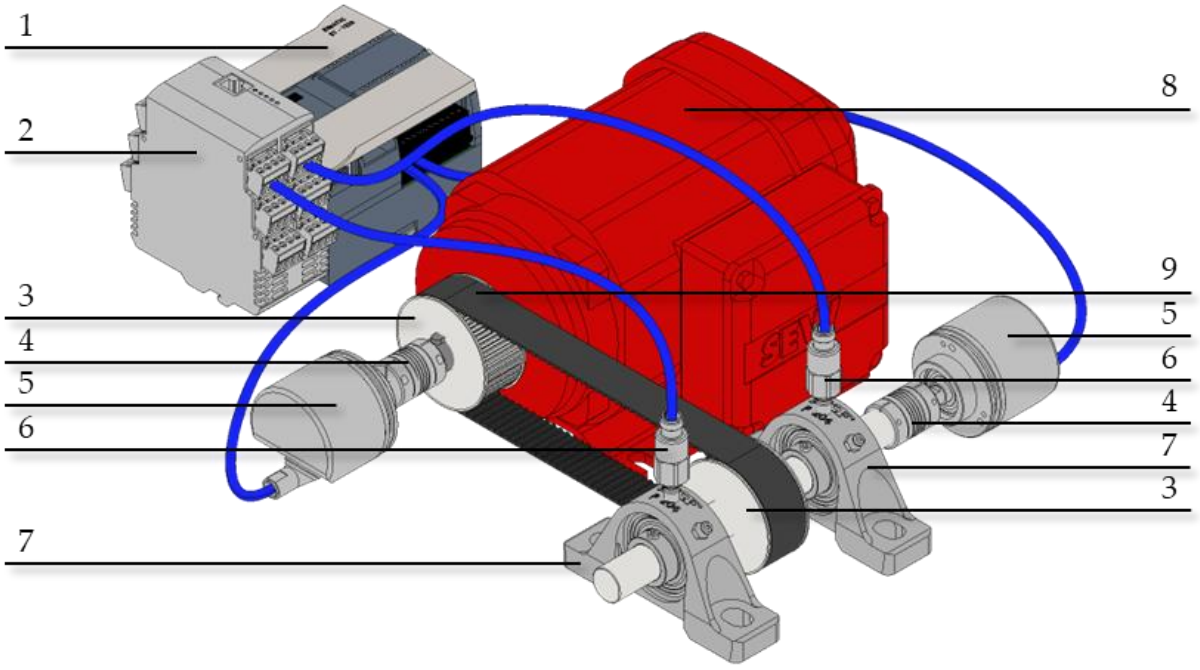

Fig. 2. Test stand composition.

Table 1. List of parts used on the test stand.

No	Element name	Type
1	Programmable Logic Controller (PLC)	SIEMENS S7-1200 CPU 1214C DC/DC/DC
2	Diagnostic electronics for vibration sensors	IFM VSE100
3	Timing pulley	T5
4	Flexible coupling for encoders	IFM E60066
5	Incremental encoder with solid shaft	IFM RV3100

No	Element name	Type
6	Acceleration sensor	IFM VSA001
7	Pillow block ball bearing units	UCP 204
8	Electric drive: motor	SEW DRS71M4
8	Electric drive: frequency converter	SEW MOVIDRIVE® MDX60B/61B
9	Timing belt	T5

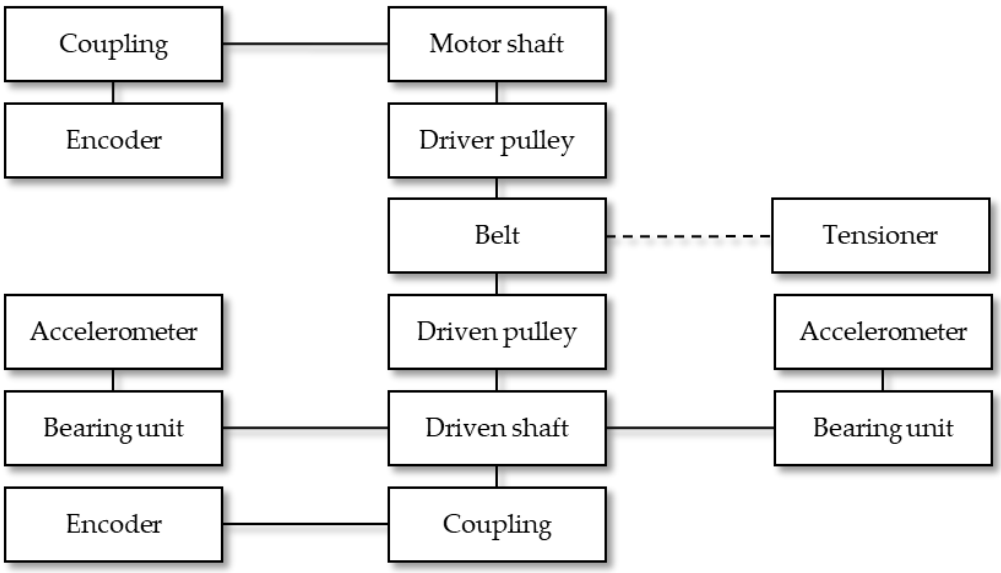

Fig. 3. Mechanical system of the test bench.

2.2. Software configuration of the test bench

The signals acquired from encoders can be processed in a PLC. There, their samples are recorded using Hight Speed Counters (HSC). The pulses generated by the encoders are counted with a resolution of 10000 pulses/rev. A program has to be created to direct the values read at a given time to a log file with e.g. a .csv extension stored in the controller memory. A time stamp can also be generated during the sample recording cycle and placed in a separate column of the log file. This procedure results in a recording frequency of approximately 20 Hz. The file can be extracted from the controller memory via the web server and stored on the networked computer for further processing. A sample of the raw data, which provided material for processing, is shown in Table 2.

Table 2. List of position measurement records.

Record	Date	UTC Time	nanosec	enc1	enc2
1	'04/19/’	'16:40:22'	11640000	0	0
2	'04/19/’	'16:40:22'	27355000	0	0
3	'04/19/’	'16:40:22'	65913000	0	0
4	'04/19/’	'16:40:22'	84437000	0	0
5	'04/19/’	'16:40:22'	101861000	0	0
6	'04/19/’	'16:40:22'	117456000	0	0
7	'04/19/’	'16:40:22'	132919000	0	0
8	'04/19/’	'16:40:22'	153544000	0	0
9	'04/19/’	'16:40:22'	169959000	0	0
...	...	...	...	...	...

An additional task of the PLC is to automatically control the drive so that all the tests can be carried out within the specified speed regime and time of each motion phase. The control signals are transmitted via PROFINET to the frequency converter controlling the electric motor.

The electronics for vibration analysis can be configured to collect signals from two accelerometers. First, it must be determined to which bearing support the vibrations are

transmitted with greater intensity, and it was at this support that the measurements were taken for the main part of the work. The measuring system allows one to generate and record mean values of samples at particular domain value (e.g. vibration frequency), gathered with 50 kHz observation frequency, every 5 seconds. It is possible to collect several vibration characteristics within a measurement planned for at least 1 minute.

Data from the device can be monitored and recorded via the IFM VES004 PC application used to save the data in files with the extension .xlsx.

The measurement system allows data to be generated in the form of a frequency spectrum, recorded at specific intervals. A section of the raw data, which constituted material for further analyses, is presented in Table 3.

Table 3. List of frequency spectrum records.

		Frequency (Hz)							
Date	**Time**	0.000000	0.254313	0.508626	0.762939	1.017253	1.271566	1.525879	...
		RMS values (rev/min)							
15.04	14:03:56	0.000000	0.000000	0.000257	0.000174	0.000120	0.000269	0.000283	...
15.04	14:04:00	0.000000	0.000000	0.000252	0.000122	0.000251	0.000249	0.000125	...
15.04	14:04:04	0.000000	0.000000	0.000411	0.000429	0.000278	0.000239	0.000035	...
15.04	14:04:08	0.000000	0.000000	0.000532	0.000043	0.000009	0.000401	0.000301	...
15.04	14:04:12	0.000000	0.000000	0.000395	0.000216	0.000263	0.000236	0.000030	...
15.04	14:04:17	0.000000	0.000000	0.000164	0.000069	0.000080	0.000113	0.000031	...
15.04	14:04:21	0.000000	0.000000	0.000016	0.000061	0.000026	0.000121	0.000201	...
15.04	14:04:25	0.000000	0.000000	0.000273	0.000124	0.000235	0.000102	0.000076	...
15.04	14:04:29	0.000000	0.000000	0.000236	0.000196	0.000362	0.000264	0.000250	...
...	...	...	...	...	...	...	...	...	...

The presented frequency values are just a sample of the whole measurement scope. The resolution is: 0.254313 Hz, which is visible in consecutive values in the Table. The resolution is related to the measurement scope in the measuring device: the higher resolution the lower scope. The resolution which enables observation of the whole spectrum of the achieved speed has been chosen. The number of decimal places was chosen to show significant changes in the values (higher and lower numbers could have presented too little information or unnecessary information).

2.3. Proposed calculation and analysis procedure

Using the angular position monitoring system, sets of samples of counted encoder pulses $e_{k=1,2}$ are collected, which are assigned UTC time stamp values.

Before the start of each analysis, the registers collecting data from the two angular position sensors are reset to zero (referenced) by subtracting the value of the first one from the subsequent samples. The number "i" is the sample number.

$$pk{=}1{,}2\ (i){=}ek{=}1{,}2\ (i){-}ek{=}1{,}2\ (1)\ [\text{pulses}] \quad (1)$$

The time stamp vector is done similarly to provide the time "t" passed from the beginning of the measurement at each sample. Additionally, nanosecond values stored in a separate column of the PLC data Table are added to UTCTime, as the controller natively does not support such accuracy in the built-in time stamp mechanism.

$$t{=}UTCTime{+}nanosec\ [mm{:}ss.000000000] \quad (2)$$

$$t(i){=}t(i){-}t(1)\ [mm{:}ss.000000000] \quad (3)$$

Sets of values representing the positions of the pulleys $p_{k=1,2}$ in moments of stabilised operation of the transmission are subjected to statistical analysis using Pearson correlation coefficient ρ_p .

$$\rho_p(p_1,p_2)=\frac{\mathrm{cov}(p_1,p_2)}{\sigma_{p_1}\sigma_{p_2}} \quad (4)$$

The direct correlation measure thus makes it possible to determine the level of convergence of the positions reached by the two pulleys. The increment of the angular position is also calculated in successive samples, excluding sample i=1, where the increment $\Delta r_{k=1,2}$ was given the value 0. In the same step, the value of the angular measure, expressed in pulses, is converted into revolutions based on the resolution of the encoder (10000 pulses/rev).

$$\Delta r_{k=1,2}(i)=\frac{p_{k=1,2}(i)-p_{k=1,2}(i-1)}{10^4}\ [\text{rev}] \quad (5)$$

The increment is also calculated with respect to samples of the time elapsed Δt and the unit is converted to the number of

minutes.

$$\Delta t(i)=t(i)-t(i-1)\ [min] \quad (6)$$

The average velocities could then be determined.

$$n_{k=1,2}=\frac{\Delta r_{k=1,2}}{\Delta t}[rev/min] \quad (7)$$

These are also subjected to the Pearson correlation analysis ρ_n, to determine which parameter is more sensitive to anomalies: position or speed.

$$\rho_n(n_1,n_2)=\frac{cov(n_1,n_2)}{\sigma_{n_1}\sigma_{n_2}} \quad (8)$$

The discrepancies in the pulley positions are then determined.

$$\Delta p=|p2-p1|\ [pulses] \quad (9)$$

The same is done for the speed of the pulleys by calculating the difference in the value of the parameter in the driving and driven pulleys.

$$\Delta n=|n2-n1|\ (rev/min) \quad (10)$$

They are subjected to statistical analysis using the RMS ratio (Root Mean Square), which is a classic measure for determining the intensity of periodic signals in drive engineering.

$$RMS_{\Delta p}=\sqrt{\frac{1}{end}\sum_{i=1}^{end}|\Delta p_i|^2}\ [pulses] \quad (11)$$

$$RMS_{\Delta n}=\sqrt{\frac{1}{end}\sum_{i=1}^{end}|\Delta n_i|^2}\ [rev/min] \quad (12)$$

The calculated values have been shown on graphs, which were subject to further analysis.

3. Results and discussion

The sources and processors of the signals used in the prototype implementation of the studied electronic and information system are shown in Fig. 4.

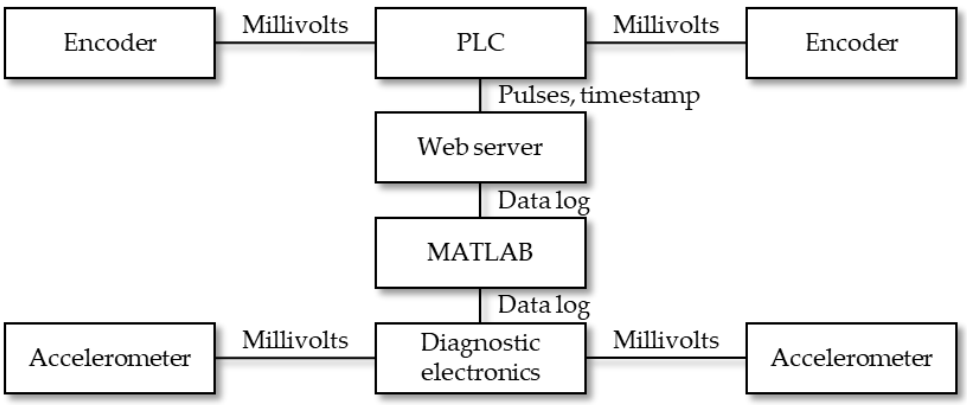

Fig. 4. Electronic and information system of the test bench.

The PLC programme created as part of the study is presented in detail in Appendix A. The files generated in the control and monitoring systems were catalogued on a networked computer and the data contained therein further processed using MATLAB software. The functions for the acquisition, processing and representation of information from external sources were used to generate appropriate numerical measures to search for a correlation model between the parameters described further. The scripts created for this purpose are included in Appendix B.

3.1. Examples of generated characteristics

In this chapter the values obtained directly from the measurements and those calculated using the formulas indicated earlier are presented in a graphical form, in time, frequency or correlation diagrams.

3.1.1. Kinematic measurements of transmission

The first available indicator of the synchronisation error is the discrepancy in positions expressed in pulses counted by encoders at both pulleys.

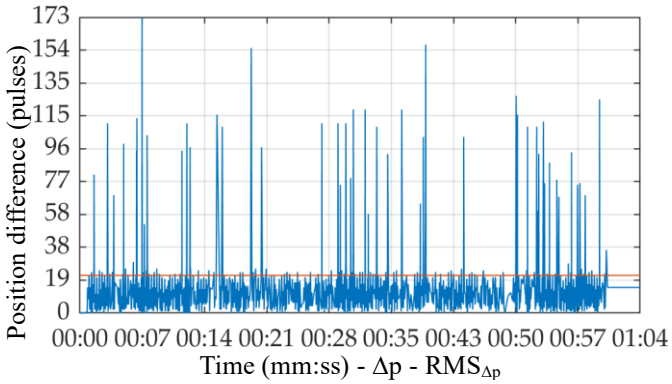

Fig. 5. Course of position difference between drive and driven pulleys, measurement with no external load, setpoint speed 200 rev/min.

Showing the position reached by pulley 1 in the event of pulley 2 reaching a given position at a given measurement sample allowed changes in the correlation of the two quantities to be shown graphically.

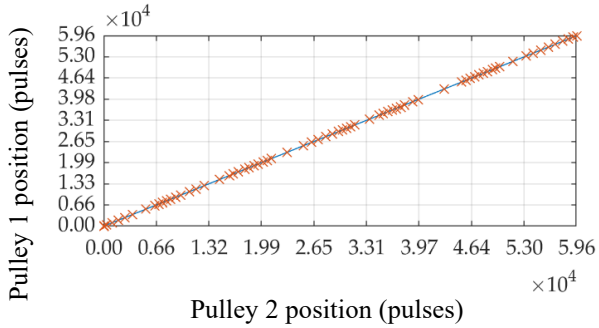

Fig. 6. Position correlation between drive and driven pulleys, measurement with no external load, setpoint speed 200 rev/min

Calculating the changes in position and time gave the possibility of mapping the instantaneous velocity in the time domain.

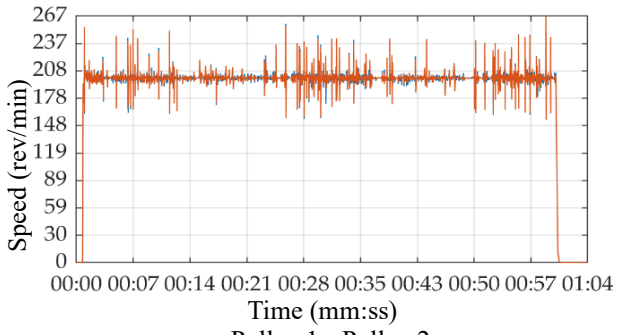

Fig. 7. Courses of rotational speed calculated for drive and driven pulleys, measurement with no external load, setpoint speed 200 rev/min.

The discrepancies in the pulley speeds are also shown in the graphs with their RMS value observed throughout the measurement.

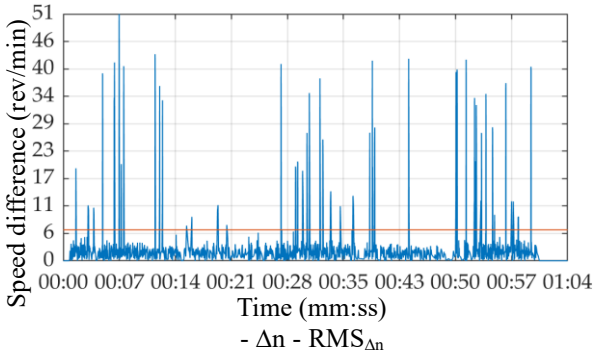

Fig. 8. Courses of speed difference between drive and driven pulleys, measurement with no external load, setpoint speed 200 rev/min.

The velocities of the two pulleys were matched against each other at all measurement samples and the correlation diagrams presented further on were obtained.

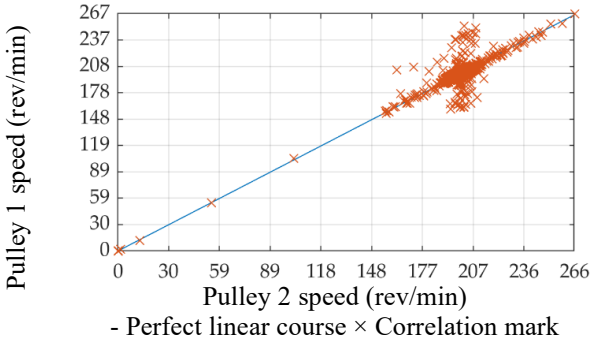

Fig. 9. Speed correlation between drive and driven pulleys, measurement with no external load, setpoint speed 200 rev/min.

Correlation measures indicate clusters of the synchronisation error according to a fixed pattern when the speed is around the set value.

3.1.2. Vibration measurements

The 3D diagrams show the level of the RMS value of the vibration velocity reached at a given frequency in the different moments of the measurement – from start-up, through the phase of stabilisation of the set speed, to stopping the movement.

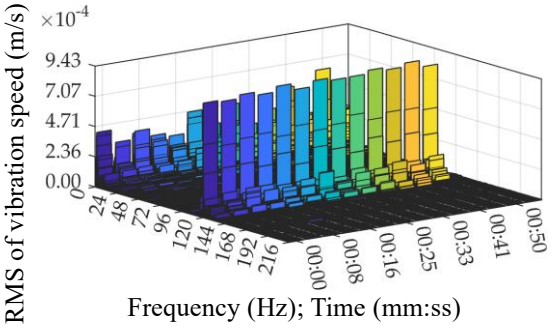

Fig. 10. RMS of vibration speed between drive and driven pulleys, measurement with no external load, setpoint speed 200 rev/min.

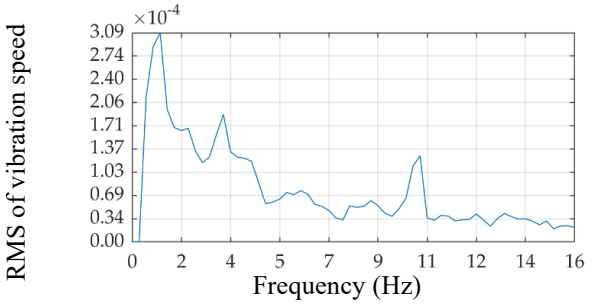

Fig. 11. RMS of vibration speed between drive and driven pulleys, measurement with no external load, setpoint speed 200 rev/min.

After averaging the values from the velocity stabilisation phase and extracting the frequency range in the vicinity of the set velocity, the results shown in Figure 11 were obtained.

A summary of the results of sections 3.1. and 3.2. is shown in Table 4.

Table 4. Summary of the results obtained during measurements.

Setpoint speed	$RMS_{\Delta p}$ (pulses)		$RMS_{\Delta n}$ (m/s)		ρ_p		ρ_n		RMS of vibration speed (m/s)	
	unloaded	loaded	unloaded	loaded	unloaded	loaded	unloaded	loaded	unloaded	loaded
200	22.0311	20.7224	6.4565	6.8325	1.0000	1.0000	0.9928	0.9859	0.0002	0.0002
400	39.4607	46.2555	13.2669	11.6556	1.0000	1.0000	0.9931	0.9855	0.0003	0.0002
600	75.4568	63.7937	22.2671	17.4194	1.0000	1.0000	0.9900	0.9941	0.0005	0.0004
800	86.4523	114.1353	24.5122	28.4121	1.0000	1.0000	0.9922	0.9900	0.0005	0.0006
1000	94.0019	123.6626	35.8082	40.7931	1.0000	1.0000	0.9905	0.9871	0.0008	0.0012
1200	101.0175	104.2828	37.2213	37.8027	1.0000	1.0000	0.9917	0.9926	0.0011	0.0032
1400	115.7593	162.3133	44.1930	46.2201	1.0000	1.0000	0.9922	0.9921	0.0016	0.0107

Further measures of the correlation no longer concern the kinematic relationship between the pulleys, but the relationship between the statistical indicators of the synchronisation error and the vibration level.

3.1.3. Correlation between the vibration level and kinematic measures

On the basis of the results obtained so far, it was possible to formulate the final measure linking the variation of the pulley synchronisation error (determined by the four previously given statistical indicators) with the variation of the vibration level. A summary of the numerical input data arranged in an ascending order with respect to the column with the effective value of the vibration velocity is shown in Table 5.

Table 5. List of load cases with its effective values.

load case, setpoint speed	RMS of vibration speed (m/s).	$RMS_{\Delta p}$ (pulses)	$RMS_{\Delta n}$ (m/s)	ρ_p	ρ_n
loaded, 200	0.0002	20.7224	6.8325	1.0000	0.9859
unloaded, 200	0.0002	22.0311	6.4565	1.0000	0.9928
loaded, 400	0.0002	46.2555	11.6556	1.0000	0.9855
unloaded, 400	0.0003	39.4607	13.2669	1.0000	0.9931
loaded, 600	0.0004	63.7937	17.4194	1.0000	0.9941
unloaded, 600	0.0005	75.4568	22.2671	1.0000	0.9900
unloaded, 800	0.0005	86.4523	24.5122	1.0000	0.9922
loaded, 800	0.0006	114.1353	28.4121	1.0000	0.9900
unloaded, 1000	0.0008	94.0019	35.8082	1.0000	0.9905
unloaded, 1200	0.0011	101.0175	37.2213	1.0000	0.9917
loaded, 1000	0.0012	123.6626	40.7931	1.0000	0.9871
unloaded, 1400	0.0016	115.7593	44.1930	1.0000	0.9922
loaded, 1200	0.0032	104.2828	37.8027	1.0000	0.9926
loaded, 1400	0.0107	162.3133	46.2201	1.0000	0.9921

The data from Table 5 were used to generate the graphs from Figure 12.

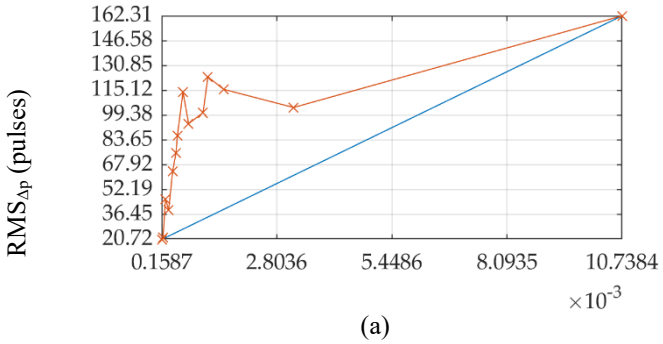

(a)

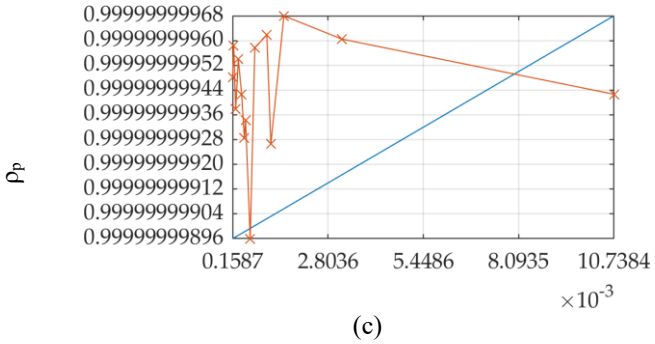

(c)

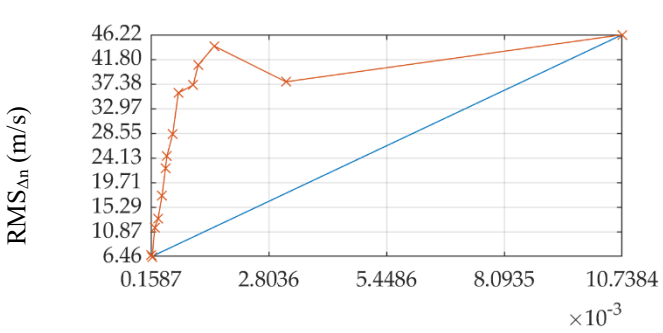

(b)

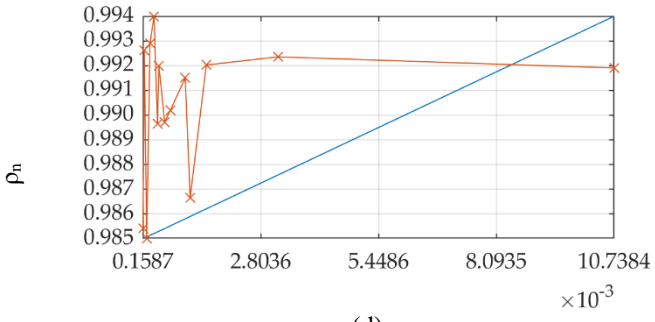

(d)

RMS of vibration speed (m/s).
- Perfect linear course × Correlation mark

Fig. 12. Comparison of courses of RMS vibration speed values of the difference in position and speed.

The final information (a base for searching correlations) is in the form of waveforms of the values of the given statistical measures observed at a given vibration level, as derived from 14 measurement trials.

4. Conclusions

The studied system is appropriate for all the specified demands and aims. The presented technology produces graphical information showing levels of the critical parameters related to the belt drive condition. By checking these several statistical measures, it supposed to be possible to find the one that most strongly reflects the synchronisation error produced by the occurrence of vibrations and other phenomena.

In parallel to the angular position measurements, the RMS value of the vibration velocity is measured. Samples of this parameter are also time-stamped to correlate them with a given phase of the drive operation. The first treatment step is to extract the average value of the measured vibration level over the entire period of stabilised motion of the mechanism. As the essence of the studied method is to compare the level of anomalies with respect to specific speeds, the frequency spectrum must be narrowed to a window around the rotational frequency obtained in a given trial. This makes it possible to directly compare the change in intensity of the analysed phenomenon (after e.g. imbalance induction) and to relate it to changes in the synchronisation error.

Additional correlation indicators may help conducting further research in the quest for extending the variety of diagnostics methods. In the modern drive technology based on frequency converters, measurement of the angular position on the drive side is becoming standard. The variation in statistical measures of asynchronism is then compared with variation in vibration levels, again using Pearson correlation coefficient. One axis shows the vibration intensity and on the other one – the statistical measures of the transmission error. Both must be observed in the same circumstances, e.g. the controlled speed and load. This analysis is supposed to be carried out several times in the whole procedure, using different (previously calculated) measures of the synchronisation error. Assuming that the result models corelating the studied phenomena would be linear, the increment on the vibration axis should be proportional to the increment on the asynchronism axis. In such a case, this would indicate a perfect correlation of the changes in the vibration level and the synchronisation error (it is presented as a reference line on the graphs in the proper section).

For industrial implementation of the authors' solution, the machine would usually only need to be fitted with an additional angular position sensor at the receiving end and coupled with a programmable logic controller (which is usually also present on machines today). Such a conclusion provides a basis for further consideration and planning experiments in many other circumstances that can be applied in the transmission operation using the experiment tools developed within this research. Thus, it will be possible to extend the field of experiments to analyse the condition of transmission operation, e.g. after the introduction of various types of unbalance or additional anomaly factors, or after changing the level of tension of the belt. All this is possible thanks to the applied assembly techniques and IT connections, as well as algorithms and automation in data acquisition and processing.

It is hypothesized that the vibration level could be identified solely from the readings of the pulley angular position or speed meters. The aim of the further research will be to determine

whether the mutual influence of these phenomena is high enough to make it possible to build models for identifying the vibration level only on the basis of angular pulley measurements [31]. What is important here is the intensity of the considered phenomena, so that with standard industrial measurement methods it is possible to observe differences in the motion of the pulleys resulting directly from the vibrations of the rotating driven element [29-30].

Further research would be aimed at recognizing the possibility of reducing sensor equipment in the area of drives while maintaining a pool of information valuable in diagnostics and correct operation of machines [32]. Vibration measurement with classical accelerometric methods requires the preparation of measurement conditions (sometimes even by surface treatment) and access to (often hidden and difficult to access without stopping and disassembling the machine) bearing components. A study is thus required to find out if there is a regular correlation between levels or forms of vibration and asynchronism in toothed belt transmissions. Another research objective could be looking for diagnostic models based on the impact of the material wear on the indicators generated with the result information technology, described in this paper.

References

1. Kagotani, M.; Aida, T.; Koyama, T.; Sato, S.; Hoshiro, T. A study on transmission characteristics of toothes belt drives. Bulletin of the JSME, 1983, Volume 26, pp. 1238-1244. https://doi.org/10.1299/jsme1958.26.1238
2. Koyama, T.; Kagotani, M.; Shibata, T.; Hoshiro, T. A study on strength of toothed belt-2nd report – Influence of Pitch Difference on Load Distribution. Bulletin of the JSME, 1979, Volume 22, pp. 982–987. https://doi.org/10.1299/jsme1958.22.982
3. Koyama, T.; Kagotani, M.; Shibata, T.; Sato, S.; Hoshiro, T. A study on strength of toothed belt-3rd report – Fatigue Strength and Features of Fracture. Bulletin of the JSME, 1979, Volume 22, pp. 988–993. https://doi.org/10.1299/jsme1958.22.988
4. Koyama, T.; Kagotani, M.; Shibata, T.; Sato, S.; Hoshiro, T. A study on strength of toothed belt-4th report – Load Distribution in Case of Considering Incomplete Meshing. Bulletin of the JSME, 1980, Volume 23, pp. 1235–1239. https://doi.org/10.1299/jsme1958.23.1235
5. Koyama, T.; Kagotani, M.; Shibata, T.; Sato, S.; Hoshiro, T. A study on strength of toothed belt-5th report – Effect of Pitch Difference on Fatigue Strength of Toothed Belt. Bulletin of the JSME, 1980, Volume 23, pp. 1240–1244. https://doi.org/10.1299/jsme1958.23.1240
6. Koyama, T.; Kagotani, M.; Shibata, T.; Sato, S.; Hoshiro, T. A study on strength of toothed belt-6th report – Behavior of Belt and Pulley Tooth at Incomplete Meshing Region. Bulletin of the JSME, 1981, Volume 24, pp. 1500–1506. https://doi.org/10.1299/jsme1958.24.1500
7. Koyama, T.; Marshek, K.M. Toothed belt drives—Past, present and future. Zahnriemenantriebe—Vergangenheit, gegenwart und zukunft. Mechanism and Machine Theory, 1988, Volume 23, pp. 227-241. https://doi.org/10.1016/0094-114X(88)90108-5
8. Köster, L. Der Zugkraftverlauf in Zahnriemenantrieben. Konstruktion, 1982, Volume 34, pp. 99-104.
9. Köster, L. Untersuchung der Kräftverhältnisse in Zahnriemenantrieben; Diss. UniBw, Hamburg, 1981.
10. Krause, W. Zahnriemengetriebe, Verlag Hüthig, Heidelberg, Germany, 1988.
11. Funk, W.; Köster, L. Problematik der Drehmomentübertragung durch Zahnriementriebe. Antriebstechnik, 1982, Volume 21, pp. 390-394.
12. Niemann, G. Maschinenelemente II, Springer-Verlag, Berlin, Germany, 1960. https://doi.org/10.1007/978-3-662-25357-1
13. Gerbert, G.; Jönsson, H.; Persson, U.; Stensson, G. Load Distribution in Timing Belts. Journal of Mechanical Design, 1978, Volume 100, pp. 208-215. https://doi.org/10.1115/1.3453902
14. Uchida, T.; Furukawa, Y.; Tomono, K.; Takahashi, H. Pitch Difference and Belt Tooth Configuration Effect on Load Distribution of Timing Belt Using FEM Analysis. Journal of engines, 1996. Volume 105, pp. 346-355. https://doi.org/10.4271/960299
15. Abrate, S. Vibrations of belts and belt drives. Mechanism and Machine Theory, 1992, Volume 27, pp. 645-659. https://doi.org/10.1016/0094-114X(92)90064-O
16. Dalgarno, K.W.; Day, A.J.; Childs, T.H.C.; Moore, R.B. Stiffness loss of synchronous belts. Composited Part B: Engineering, 1998, Volume 29, pp. 217-222. https://doi.org/10.1016/S1359-8368(97)00033-4
17. Alspaugh, D.W. Torsional vibration of a moving band. Journal of the Franklin Institute, 1967. Volume 283, pp. 328-338. https://doi.org/10.1016/0016-0032(67)90047-6
18. Childs, T.H.C.; Parker, I.K. Power transmission by flat, V and timing belts. Tribology Series, 1989, Volume 14, pp. 133-142. https://doi.org/10.1016/S0167-8922(08)70187-1
19. Belofsky, H. On the theory of power transmission by a flat, elastic belt. Wear, 1973. Volume 25, pp. 73-84. https://doi.org/10.1016/0043-

1648(73)90122-1
20. Chowdhurry, S.; Yedavalli, R.K. Dynamics of belt-pulley-shaft systems. Mechanism and Machine Theory, 2016, Volume 98, pp. 199-215. https://doi.org/10.1016/j.mechmachtheory.2015.11.011
21. Wenbo, L.; Zhenxiang, X. Flexural fatigue life prediction of a tooth V-belt made of fiber reinforced rubber. International Journal of Fatigue, 2018. Volume 111, pp. 269-277. https://doi.org/10.1016/j.ijfatigue.2018.02.025
22. Khazaee, M.; Banakar, A.; Ghobadian, B.; Mirsalim, M.A.; Minaei, S.; Jafari, S.M. Detection of inappropriate working conditions for the timing belt in internal combustion engines using vibration signals and data mining. Proceedings of the Institution of Mechanical Engineers, Part D: Journal of Automobile Engineering, 2017. Volume 231, pp. 418-432. https://doi.org/10.1177/0954407016641323
23. Johanesson, T. Synchronous belt mechanics and durability – An investigation towards life prediction. Doktorsavhandlingar vid Chalmers Tekniska Hogskola, 2003. Volume 1953, pp. i+1-67.
24. Bucchi, F.; Frendo, F. Enhanced brush model for the mechanics of power transmission in flat belt drives under steady–state conditions: Effect of belt elasticity. Mechanism and Machine Theory, 2020, Volume 153. https://doi.org/10.1016/j.mechmachtheory.2020.103998
25. Bucchi, F.; Frendo, F. Validation of the brush model for the analysis of flat belt transmissions in steady-state conditions by finite element simulation. Mechanism and Machine Theory, 2022, Volume 167. https://doi.org/10.1016/j.mechmachtheory.2021.104556
26. Kycyku, A.; Likaj, R.; Hamidi, B. Modelling and Analysis of Nominal Conveying Ability for the Toothed Belt with STD Profile. IFAC-PapersOnLine, 2016. Volume 49, pp. 243-246. https://doi.org/10.1016/j.ifacol.2016.11.059
27. Zhang, L.; Zy, J.W. Modal analysis of serpentine belt drive systems. Journal of Sound and Vibration, 1999. Volume 222, pp. 259-279. https://doi.org/10.1006/jsvi.1998.2078
28. Fehsenfeld, M.; Kühn, J.; Wielitzka, M.; Ortmaier, T. Tension Monitoring of Toothed Belt Drives Using Interval-Based Spectral Features. IFAC-PapersOnLine, 2020. Volume 53, pp. 738-743. https://doi.org/10.1016/j.ifacol.2020.12.824
29. Childs, T.H.C.; Parker, I.K.; Day, A.J.; Coutzoucos, A.; Dalgarno, K.W. Paper XII (ii) Tooth Loading and Life of Automotive Timing Belts. Tribology Series, 1991. Volume 18, pp. 341-348. https://doi.org/10.1016/S0167-8922(08)70150-0
30. Childs, T.H.C.; Dalgarno, K.W.; Hojjati, M.H.; Tutt, M.J.; Day, A.J. The meshing of timing belt teeth in pulley grooves. Pro-ceedings of the Institution of Mechanical Engineers, Part D: Journal of Automobile Engineering, 1997. Volume 211, pp. 205-218. https://doi.org/10.1243/0954407971526362
31. Bucchi, F.; Frendo, F. "Brush model" for the analysis of flat belt transmissions in steady-state conditions. Mechanism and Machine Theory, 2020, Volume 143. https://doi.org/10.1016/j.mechmachtheory.2019.103653
32. Firbank, T.C. Mechanics of the belt drive. International Journal of Mechanical Science, 1970, Volume 12, pp. 1053-1063. https://doi.org/10.1016/0020-7403(70)90032-9

Appendix A

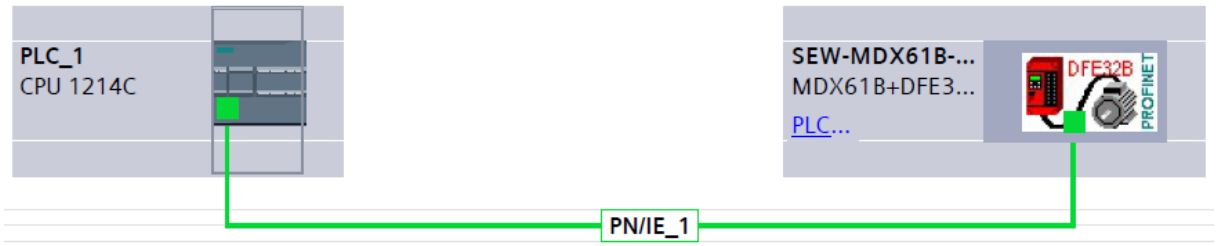

Network 1:

Network 2:

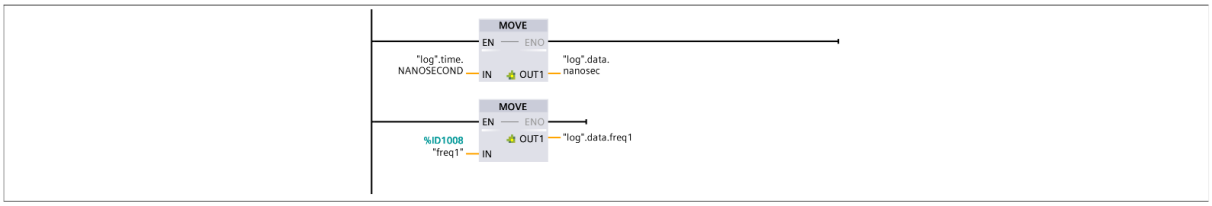

Network 3:

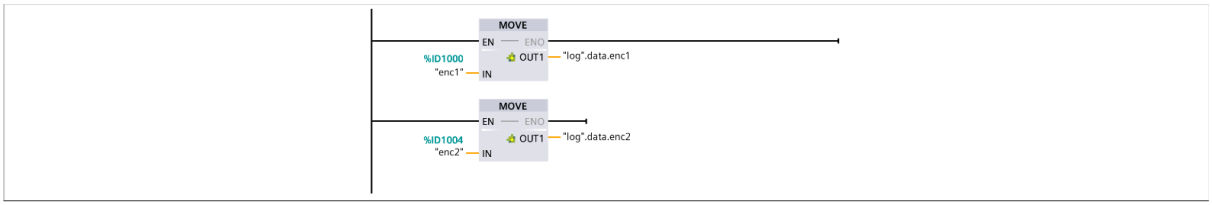

Network 4:

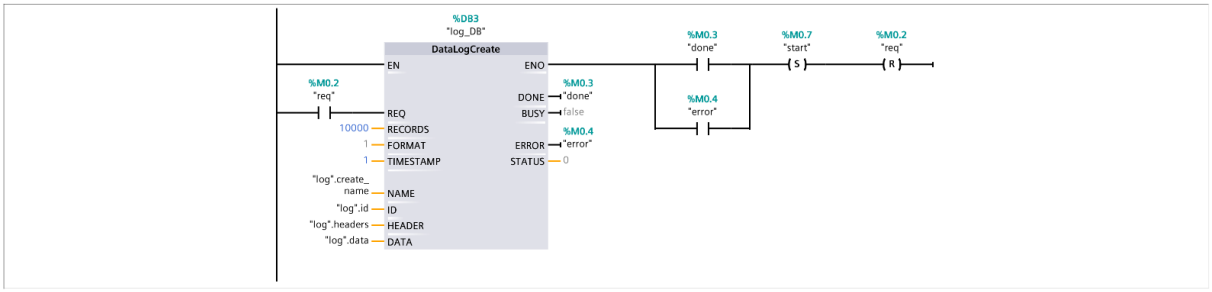

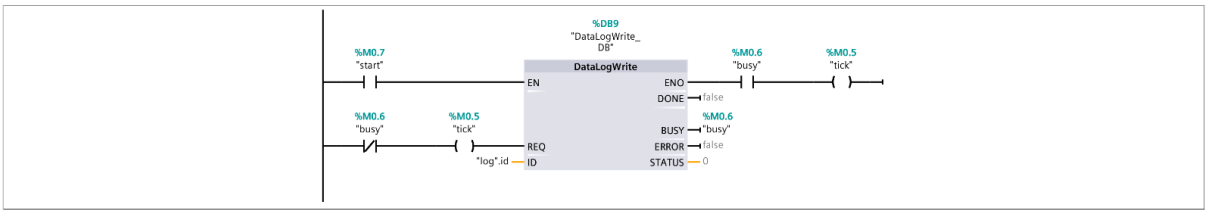

Network 6:

Network 6:

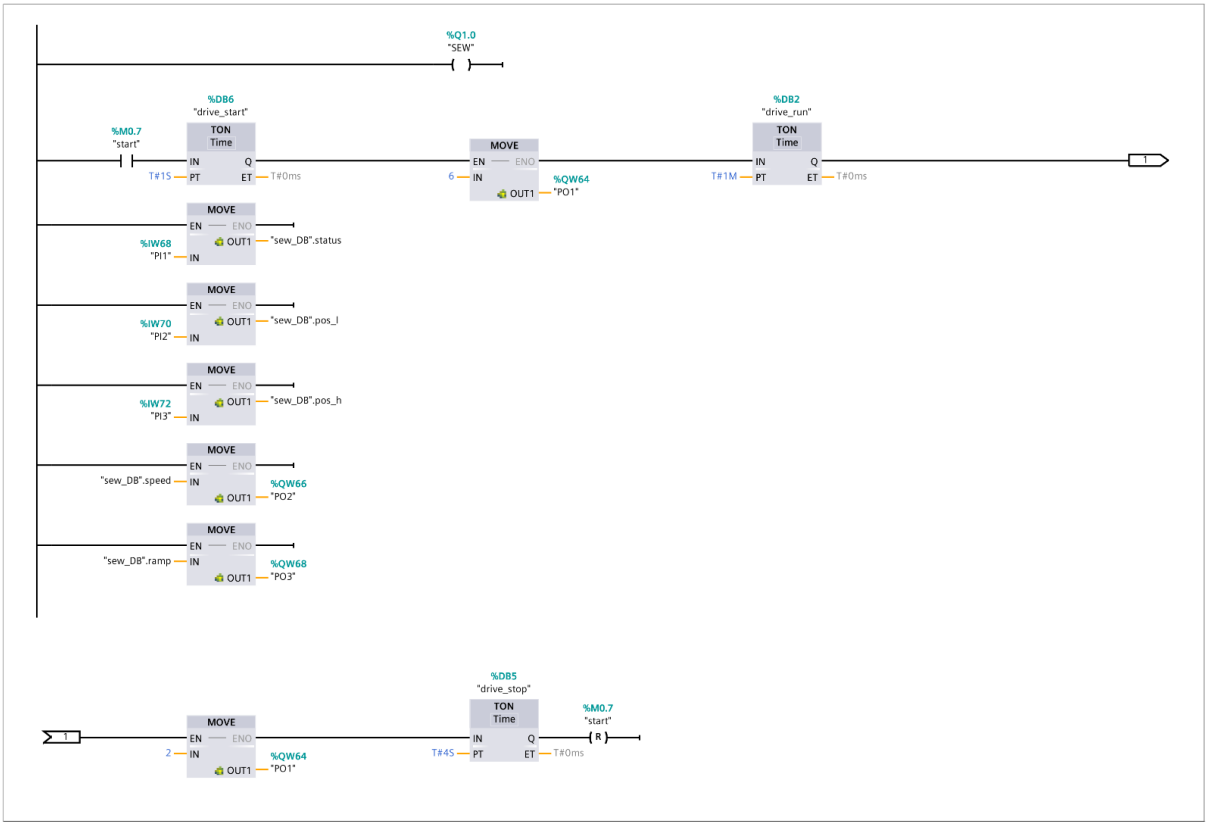

Network 7:

Appendix B

```
close all
clear
clc
c=["unloaded" "loaded"];
n=200:200:1400;
Table1=zeros(7,10);
vt(1,1)={'string'};
vt(1,2:6)={'double'};
```

```
    Table2=Table('Size',[14 6],'VariableTypes',vt);
    for k=1:length(c)
        for j=1:length(n)
            di=readTable(c(k)+"/"+n(j)+"/log.csv");
            t=di.UTCTime+seconds(di.nanosec/1e9);
            t=t-t(1);
            i=2:length(t);
            p1=di.enc1(1)-di.enc1;
            p2=di.enc2(1)-di.enc2;
            dp=abs(p2-p1);
            rmsp=repelem(rms(dp),length(t))';
            Table2(j+7*(k-1),1)={c(k)+", "+n(j)};
            Table1(j,k)=rmsp(1);
            Table2(j+7*(k-1),3)={rmsp(1)};
            rp=corrcoef(p1,p2);
            Table1(j,k+4)=rp(2,1);
            Table2(j+7*(k-1),5)={rp(2,1)};
            dt=t(i)-t(i-1);
            dt=minutes([0;dt]);
            dr1=(p1(i)-p1(i-1))/1e4;
            dr1=[0;dr1];
            dr2=(p2(i)-p2(i-1))/1e4;
            dr2=[0;dr2];
            n1=dr1./dt;
            n1(1)=0;
            n2=dr2./dt;
            n2(1)=0;
            dn=abs(n2-n1);
            rmsn=repelem(rms(dn),length(t))';
            Table1(j,k+2)=rmsn(1);
            Table2(j+7*(k-1),4)={rmsn(1)};
            rn=corrcoef(n1,n2);
            Table1(j,k+6)=rn(2,1);
            Table2(j+7*(k-1),6)={rn(2,1)};
            opts =
detectImportOptions(c(k)+"/"+n(j)+"/spectrum.xlsx",'Sheet','Sensor 1');
            opts = setvartype(opts,'Var2',{'datetime'});
            di2=readTable(c(k)+"/"+n(j)+"/spectrum.xlsx",opts);
            clear opts
            t2=Table2array(di2(2:size(di2),2));
            t2=t2-t2(1);
            t2.Format='mm:ss';
            f=Table2array(di2(1,3:size(di2,2)));
            v=Table2array(di2(2:size(di2,1),3:size(di2,2)));
            vic=length(t2)/2;
```

```
            vi1=round(vic-0.25*length(t2));
            vi2=round(vic+0.25*length(t2));
            vm=mean(v(vi1:vi2,:));
            fn=n(j)/60;
            fd=abs(f-fn);
            fic=find(fd==min(fd));
            Table1(j,k+8)=vm(fic);
            Table2(j+7*(k-1),2)={vm(fic)};
            fi1=fic-50;
            if fi1<1
                fi1=1;
            end
            fi2=fic+50;
            if fi2>length(f)
                fi2=length(f);
            end
            vr=vm(fi1:fi2);
            fr=f(fi1:fi2);
            fig2(t,n1,n2,'mm:ss','%.0f','-',"n, "+c(k)+", "+n(j)+" rpm",9);
            fig2(t,dp,rmsp,'mm:ss','%.0f','-',"dp, "+c(k)+", "+n(j)+" rpm",9);
            fig2(t,dn,rmsn,'mm:ss','%.0f','-',"dn, "+c(k)+", "+n(j)+" rpm",9);
            fig2(n1,n1,n2,'%.0f','%.0f','x',"rn, "+c(k)+", "+n(j)+" rpm",9);
            fig2(p1(1:100),p1(1:100),p2(1:100),'%.2f','%.2f','x',"rp, "+c(k)+",
"+n(j)+" rpm",9)
            fig1(fr,vr,"vr, "+c(k)+", "+n(j)+" rpm");
            fig3(t2,f,v,"v ,"+c(k)+", "+n(j)+" rpm");
        end
    end
    Table2=sortrows(Table2,2);
    array2=Table2array(Table2(:,2:6));
    rmspn=normalize(array2(:,1),"range",[min(array2(:,2)) max(array2(:,2))]);
    rmsnn=normalize(array2(:,1),"range",[min(array2(:,3)) max(array2(:,3))]);
    rpn=normalize(array2(:,1),"range",[min(array2(:,4)) max(array2(:,4))]);
    rnn=normalize(array2(:,1),"range",[min(array2(:,5)) max(array2(:,5))]);
    fig2(array2(:,1),rmspn,array2(:,2),'%.4f','%.2f','x',"vrmsp",4);
    fig2(array2(:,1),rmsnn,array2(:,3),'%.4f','%.2f','x',"vrmsn",4);
    fig2(array2(:,1),rpn,array2(:,4),'%.4f','%.2f','x',"vrp",4);
    fig2(array2(:,1),rnn,array2(:,5),'%.4f','%.2f','x',"vrn",4);

    function fig1 (x,y,t)
    plot(x,y);
    xlim([x(1) x(length(x))]);
    ylim([min(y) max(y)]);
    xtickformat('%.0f');
    ytickformat('%.2f');
```

```
    a=gca;
    set(a,'XTick',a.XLim(1):(a.XLim(2)-
a.XLim(1))/9:a.XLim(2),'YTick',a.YLim(1):(a.YLim(2)-a.YLim(1))/9:a.YLim(2));
    export(a,t);

    function fig2(x,y1,y2,f1,f2,s2,t,l)
    plot(x,y1);
    hold on
    plot(x,y2,s2);
    xlim([min(x) max(x)]);
    ylim([min([y1;y2]) max([y1;y2])]);
    xtickformat(f1);
    ytickformat(f2);
    a=gca;
    set(a,'XTick',a.XLim(1):(a.XLim(2)-
a.XLim(1))/l:a.XLim(2),'YTick',a.YLim(1):(a.YLim(2)-
a.YLim(1))/9:a.YLim(2),'XTickLabelRotation',0);
    export(a,t);

    function fig3(x,y,z,t)
    bar3(y,z');
    ylim([y(1) y(length(y))]);
    zlim([min(min(z)) max(max(z))]);
    ytickformat('%.0f');
    ztickformat('%.2f');
    a=gca;
    set(a,'XTick',1:2:length(x),'XTickLabel',string(x(1):2*x(end)/(length(x)-
1):x(end)),'YTick',a.YLim(1):(a.YLim(2)-
a.YLim(1))/9:a.YLim(2),,'ZTick',a.ZLim(1):(a.ZLim(2)-a.ZLim(1))/4:a.ZLim(2));
    axis normal
    export(a,t);

    function export(a,t)
    box(a,'on');
    set(gcf,'Units','centimeters','Position',[2 1 8.99
8.99*(9/16)],'Resize','off');
    set(a,'FontName','Palatino Linotype','FontSize',10,'XGrid','on','YGrid','on');
    a.Position(1)=a.TightInset(1);
    a.Position(2)=a.TightInset(2);
    a.Position(3)=1-a.Position(1)-a.TightInset(3);
    a.Position(4)=1-a.Position(2)-a.TightInset(4);
    exportgraphics(gcf,t+".png","Resolution",300);
    delete(gcf);
```